J. Phys. D: Appl. Phys. 25 (1992) 106–112. Printed in the UK

Raman scattering of proton exchanged $LiNbO_3$ waveguides

I Savatinova†, S Tonchev†, E Popov†, E Liarokapis‡ and C Raptis‡

† Institute of Solid State Physics, Bulgarian Academy of Sciences, Blvd Lenin 72, Sofia 1784, Bulgaria
‡ Physics Department, National Technical University of Athens, GR 157 73 Zografou, Greece

Received 22 April 1991, in final form 24 October 1991

Abstract. Proton exchanged $LiNbO_3$ waveguides are studied using Raman spectroscopy. Depending on the waveguide mode, the spectra resemble those of pure $LiNbO_3$ at high temperatures. A characteristic peak appears at 69 cm^{-1} which is probably due to second-order Raman scattering but strongly associated with the presence of protons. It is proposed that the change in the Raman spectra is due to the coexistence of the ferroelectric and paraelectric phases of $LiNbO_3$ at room temperature, induced by the proton exchange deformations on the lattice.

1. Introduction

$LiNbO_3$ optical waveguides exhibit unusual physical properties and are of great importance for optical applications. The proton exchange process, $H^+ \leftrightarrow Li^+$, is a new but quite popular technique for the fabrication of such waveguides. The guide layers have the advantages of extraordinarily high refractive index ($\Delta n = 0.12$ at $\lambda = 633$ nm) and optical damage resistance (Wong 1988).

In spite of the numerous investigations of layer composition, the mechanism of the exchange process and the structure of the guide layers is not completely clear. It is widely accepted that the refractive index increase, which causes the lightguiding effect, is connected with OH^- formation (Canali *et al* 1986). Given that IR absorption is very sensitive to H^- (OH^-) concentration in the crystal, particular attention has been paid (in IR spectroscopic studies) to the spectral region around the OH-stretching vibrations (Canali *et al* 1986, Richter *et al* 1989, Savatinova *et al* 1990a). To our knowledge the present work is the first attempt to achieve better understanding of the characteristics of $Li_{1-x}H_xNbO_3$ waveguides by applying Raman spectroscopy.

Conventional Raman scattering of thin films can give important information about their structure and vibrational behaviour; however, considerable difficulties have to be overcome. In recent years the waveguide Raman technique has been developed (Rabolt and Swalen 1988) in conjuction with the progress of integrated optics. Optical waveguiding allows a great amount of light to be trapped inside the film and this results in a large enhancement of the Raman scattering intensity. Until now the waveguide Raman technique has been successfully demonstrated for polymer and organic thin films (Miller *et al* 1987, Rabolt *et al* 1980). In this work, Raman scattering results from single-crystal thin layers are reported for the first time.

2. Samples and experiments

Commercially available (for device fabrication) single crystals of $LiNbO_3$ were used. Several oriented plates with dimensions 2 x 10 x 20 mm were cut and polished with the two larger faces perpendicular to the optical axis z. Proton-substituted guide layers were produced by immersing z-cut $LiNbO_3$ plates in a melt of benzoic acid with 1% of lithium benzoate. The exchange process, $H^+ \leftrightarrow Li^+$, was performed at 230 °C for various time intervals.

The majority of the waveguides were supporting 1–3 modes at $\lambda = 633$ nm, the mode number being approximately two times greater at $\lambda = 441.6$ nm. The laser beam was coupled into the guide layers by a prism of $SrTiO_3$ ($n = 2.3887$). The measured effective mode indices n_{eff} of two typical waveguides are given in table 1.

The inverse WKB procedure (Kolosovskii *et al* 1981) was used to obtain the refractive index profile of the layers. Since the reconstruction of the index profile needs a number of modes $N \geqslant 4$, the waveguides were also measured at the shorter wavelength of $\lambda = 441.6$ nm when necessary. Figure 1 shows the result for the sample Z09. It is seen that the usually accepted step-like form for this type of waveguide is a rather good approximation. The guide parameters, that is, the index

0022-3727/92/010106+07$03.50

Table 1. Mode characteristics and parameters of $Li_{1-x}H_xNbO_3$ waveguides.

Sample	Exchange time (h)	Mode spectrum $\lambda = 633$ nm	Δn	$\lambda = 441.6$ nm	Δn	W (μm)
Z09	12	$n_{eff,0} = 2.3038$ $n_{eff,1} = 2.2763$ $n_{eff,2} = 2.2322$	0.117	$n_{eff,0} = 2.4342$ $n_{eff,1} = 2.4192$ $n_{eff,2} = 2.3961$ $n_{eff,3} = 2.3641$ $n_{eff,4} = 2.3238$	0.150	1.4
Z08	3	$n_{eff,0} = 2.2932$ $n_{eff,1} = 2.2312$	0.115			0.9

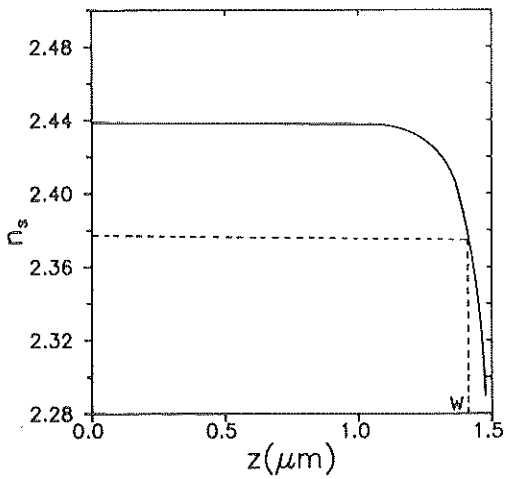

Figure 1. Refractive index profile of the sample Z09 for the 441.6 nm laser wavelength.

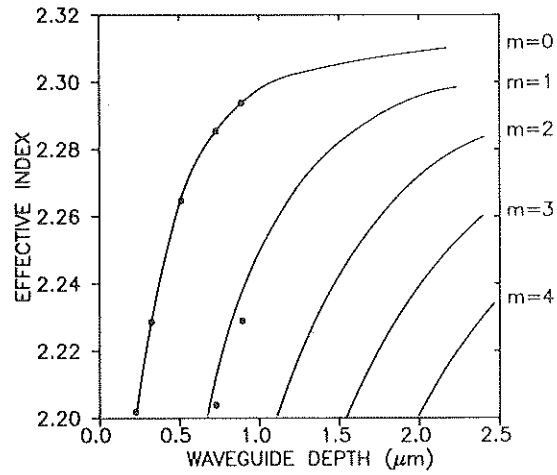

Figure 2. Dispersion curves for H:$LiNbO_3$ waveguides formed in benzoic acid–lithium benzoate (●, data points).

change $\Delta n = n_s - n_b$ (where n_b, n_s are the bulk and surface extraordinary refractive indices) and the waveguide thickness W (characterized by a refractive index change of $\Delta n_{max}/2$), were estimated and their values are also given in table 1. In figure 2 the dispersion curves for the waveguides are given, calculated for $\lambda = 647$ nm. Based on these curves, the cut-off depth for each guided mode can be extracted.

Raman scattering was excited by the 647.1 nm line of a Kr^+ laser and the 514.5 nm line of an Ar^+ laser. SPEX and DFS-12 double monochromators and the standard photon counting systems were used to detect the Raman signal. Typical laser beam powers measured in front of the input prism were $\sim$ 100 mW. The trace of the laser light in the waveguide was parallel to the entrance slit in a 90° geometry (figure 3).

As the proton-exchange produces an extraordinary refractive index change Δn_e, only light with TM polarization can be guided in Z-cut waveguides. As the X and Y directions are equivalent in uniaxial crystals we did not use an analyser in front of the entrance slit. In this situation, we were able to obtain only the $y(z\,^x_y)z$ scattering geometry, i.e. to observe only E phonons associated with the following Raman tensors

$$E(X) = \begin{pmatrix} 0 & -c & -d \\ -c & 0 & 0 \\ -d & 0 & 0 \end{pmatrix}$$

and

$$E(Y) = \begin{pmatrix} c & 0 & 0 \\ 0 & -c & d \\ 0 & d & 0 \end{pmatrix}.$$

At room temperature $LiNbO_3$ is ferroelectric and belongs to the C^6_{3v} space group (rhombohedral phase). At a temperature of $T_c \approx 1200\,^\circ$C (Bergman *et al* 1968, Gallagher and O'Brien 1985) it undergoes a phase transition to the D^6_{3d} structure and becomes paraelectric. In the ferroelectric phase, 13 Raman active vibrations ($4A_1 + 9E$) have been observed (Yang *et al* 1987, Kaminow and Johnston 1967) in agreement with the predictions

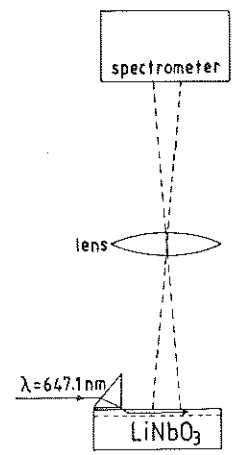

Figure 3. Experimental set-up for waveguide Raman measurements.

of theory. Given that most of the phonons are polar, the degeneracy between TO–LO vibrations is lifted, so a large number of Raman lines can be seen. In addition most of the phonons vary in frequency depending on the direction of their propagation relative to the optical axis. In the high-temperature paraelectric phase only 5 ($1A_{1g}$ + $4E_g$) Raman active phonons are predicted by group theory. The paraelectric crystal structure has a centre of inversion and the phonons are non-polar, i.e. there is no TO–LO splitting. Given that the Curie point T_c is unusually high and only slightly lower than the melting point of the crystal (T_m = 1260 °C), the available information on Raman scattering in the paraelectric phase of $LiNbO_3$ is limited and lacks clarity (Voronko *et al* 1987). Two different models have been proposed to interpret the phase transition from paraelectric to ferroelectric in $LiNbO_3$ and its isomorphous $LiTaO_3$. One of them (Johnston and Kaminow 1968, Okamoto *et al* 1985) suggests a displacive mechanism, i.e. the sublattices of the positive Li^+ and Nb^{5+} ions moving relative to the sublattice of the O^{2-} anions, the displacements determining the direction of the spontaneous polarization P_s in the ferroelectric phase. Chowdhury *et al* (1978) and Penna *et al* (1976a) support an order–disorder type of transition. Both models consider the lithium ions as located (in fixed or statistically average positions) within the oxygen planes at $T \geqslant T_c$, while at $T \leqslant T_c$ they are in octahedral sites between those planes (Abrahams *et al* 1966, 1973, Weis and Gaylord 1985).

3. Data analysis and discussion

Figure 4 shows the $y(z\bar{x}_y)z$ Raman spectrum (in the region 0–900 cm^{-1}) of sample Z09 for three different guide modes m = 0, 1 and 2. Also in the same figure, the spectrum of the pure unexchanged substrate (bulk material) is shown, obtained with a conventional 90° scattering geometry. Therefore, a comparison between the Raman spectra of a 1.4 μm protonated layer and bulk $LiNbO_3$ single crystal can be carried out. The spectrum of the lattice vibrations with frequencies less than 900 cm^{-1} is strong and comparable to that obtained from the bulk material by the classical method. On the other hand, in the high-frequency region our experiments have shown that the Raman active OH^- stretching modes are very weak and non-informative.

Bearing in mind the fabrication conditions followed in the present study and the related published data (Rice 1986), the parameter x characterizing the proton content in our samples can be assumed in the range $0.5 \leqslant x \leqslant 0.75$. It is apparent that for such a degree of substitution the perturbations in the Raman spectrum are quite strong. All the waveguide spectra of figures 4(*a*)–(*c*) contain narrow lines observed in the spectrum of the bulk (figure 4(*d*)) but most of them are superimposed on much broader peaks (see the features at about 155, 250, 350 and 610 cm^{-1}). In addition, a new strong band at 69 cm^{-1} appears in the waveguide spectra; also another weak band is observed at 660 cm^{-1}

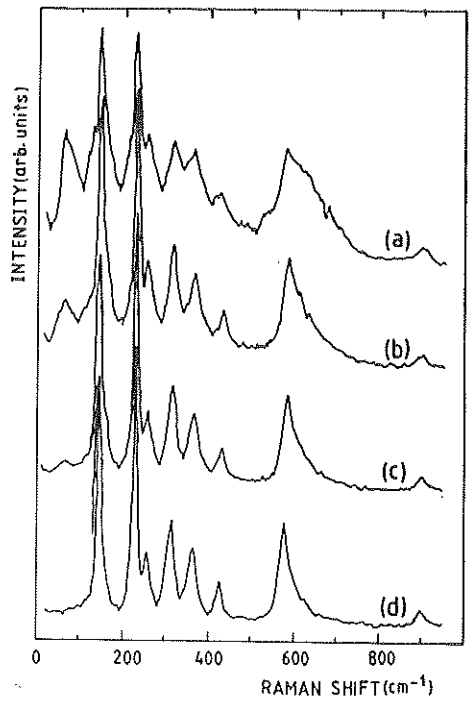

Figure 4. $y(z\bar{x}_y)z$ Raman scattering of a proton exchanged $LiNbO_3$ waveguide: (*a*) m = 0, (*b*) m = 1, (*c*) m = 2, (*d*) Raman spectrum of a single $LiNbO_3$ crystal obtained with the 90°-scattering geometry (bulk spectrum).

in the spectrum of the m = 0 mode. With increasing mode number m, the above perturbations become less pronounced and the spectrum gradually evolves into the bulk form with the intensity of the 69 cm^{-1} band decreasing practically down to zero. The origin of this peak at 69 cm^{-1} is not quite clear. A similar peak has been weakly observed in bulk $LiNbO_3$ by Claus *et al* (1972) and Penna *et al* (1976b) and in its isomorphous $LiTaO_3$ by Raptis (1988) at room temperature, and attributed to a two-phonon (difference) scattering process (Claus *et al* 1972, Raptis 1988), as it appears in all polarization configurations and its intensity increases with temperature at a rate well above that of the first-order normal modes of the crystal (Raptis 1988). The corresponding peak in $LiTaO_3$ becomes quite strong as T_c is approached and is retained, in a pronounced way, in the paraelectric phase. A similar temperature dependence investigation for the 69 cm^{-1} band of $LiNbO_3$ is planned as well as for the rest of the Raman-active modes. Comparison of our spectra of the m = 0 mode and that of pure (bulk) $LiNbO_3$ at high temperatures (Voronko *et al* 1987) reveals an overall similarity in the spectral forms, although the peaks in our spectrum appear narrower. Unfortunately, the resolution of the spectra in Voronko *et al* (1987) is not good enough to assess whether the bands at 69 and 660 cm^{-1} emerge at high temperatures, as is the case with the low-frequency band of pure (bulk) $LiTaO_3$ (Raptis 1988).

In the spectrum of the m = 0 mode (figure 4(*a*)) both peaks at 69 and 660 cm^{-1} are enhanced in intensity (compared with the spectra of the m = 1 and m = 2 modes) while the first-order Raman peaks (normal lattice vibrations) are broadened and become less

intense. It is apparent that these characteristics become less pronounced with increasing mode number, thus providing evidence that the Raman scattering is influenced by the presence of protons and a correlation between the Raman spectrum and mode m exists.

The intensity of Raman scattering in a planar waveguide is proportional to the optical intensity of the travelling mode. The optical field of the fundamental mode is localized mainly in the guide layer, with the degree of localization depending on the thickness of the guide. The optical fields of the higher-order modes penetrate more and more deeply into the substrate where the proton concentration is negligible. This is the reason for the intensity decrease of the 69 cm^{-1} band from mode $m = 0$ to mode $m = 2$ observed in figure 4. The decrease is more progressive than that expected for a three-mode waveguide with a step-like index profile. The accelerated light leakage is characteristic of a graded index distribution rather than of that presented in figure 1. However, the profile reconstruction is based on a limited amount of information (a few values of mode indices) in which some deviations from the real situation cannot be excluded.

It has recently been established that at high H concentrations, a very thin (0.1–0.2 μm) perovskite $HNbO_3$ layer is formed on the very top of the protonated layers (Richter *et al* 1989). The top layer has a different (cubic) symmetry and a refractive index higher than that of the basic exchanged layer. In principle, the presence of a superlayer could be the reason for the perturbation observed in the spectra (Noda *et al* 1978). The effect is expected to be stronger in X-cut samples with waveguides formed in pure acidic media, than in Z-cut samples formed at a reduced rate of proton exchange (addition of lithium benzoate) as is the case in our experiment. In any case, we have checked this point carefully using the sample Z08. The following experiment was performed. The sample was polished gradually (in a step-like manner), each time taking away about 0.1 μm of the surface and then the values of effective indices $n_{\mathrm{eff},m}$ of the remaining waveguide layer were measured at $\lambda = 647$ nm. These values are indicated as experimental points in figure 2. From the dispersion curves we were able to determine the corresponding guide thickness w or the thickness of the polished layer d_p after every polishing step, the Raman spectrum of the $m = 0$ mode was registered and the effective mode index $n_{\mathrm{eff},0}$ was measured. In order to understand this experiment let us consider the behaviour of the $m = 0$ mode in waveguides with different depth. If the guide thickness is large enough ($w/\lambda \sim 10$), the optical field of the fundamental mode is confined almost entirely to the interior of the film. When the film thickness is reduced to $w/\lambda \sim 1$, the field is compressed. The peak power increases but at the same time the field begins to spread out into the substrate. In very thin films, the spreading into the substrate becomes dominant resulting in a leaky mode.

Assuming a refractive index distribution like that shown in figure 1 and following the numerical calculation procedure described by Savatinova *et al* (1988), the optical intensity I_{opt} of the $m = 0$ mode after each polishing step has been obtained, and the results are illustrated in figure 5. The Raman scattering strength of the waveguide (after each polishing step) is determined from the part of I_{opt} which extends in the region $z \leqslant w$. The dependence of this fraction of I_{opt} on the thickness of the polished layer d_p is given in figure 6.

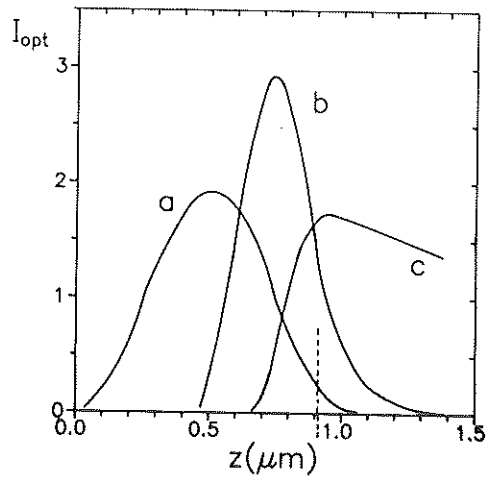

Figure 5. Optical intensity distribution of the fundamental mode of the sample Z08 at different polishing stages: curve a, $d_p = 0$ μm, curve b, $d_p = 0.45$ μm, curve c, $d_p = 0.6$ μm.

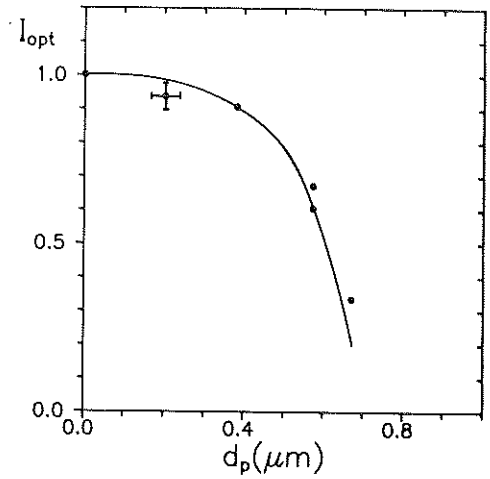

Figure 6. Optical intensity of the $m = 0$ mode (I_{opt}) versus thickness of the polished layer d_p; data points correspond to the Raman intensity of the 69 cm^{-1} band normalized to the intensity of the 155 cm^{-1} phonon.

To characterize the spectral changes more quantitatively we have considered the intensity of the 69 cm^{-1} band which is very much influenced by the experimental conditions. One could alternatively consider the peak at 660 cm^{-1} which shows similar characteristics to the 69 cm^{-1} peak but the latter is more convenient for measurements because of its isolation (figure 4). The integrated intensity of the band was measured relative to that of the 155 cm^{-1} band which, as a whole, was rather constant. The dependence of the normalized intensity of the 69 cm^{-1} band on the thickness of the

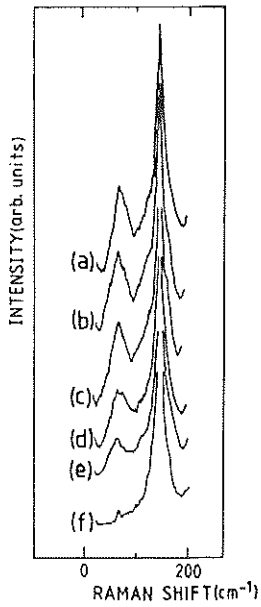

Figure 7. Low-frequency Raman scattering of the sample Z08: (*a*) after the proton exchange, (*b*), (*c*), (*d*) and (*e*) after consecutive polishings of very thin layers from the surface (see figure 6), (*f*) bulk spectrum.

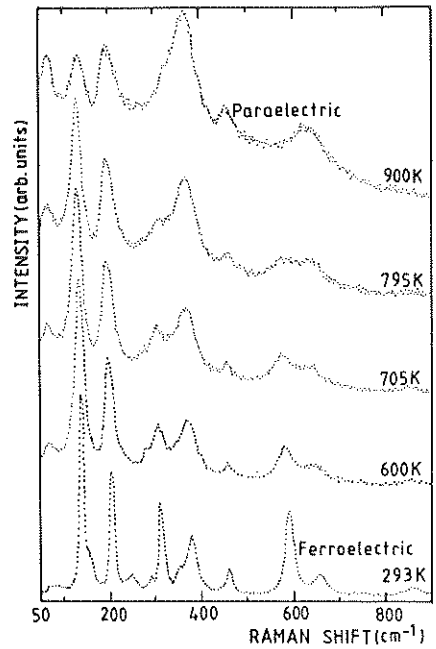

Figure 8. Temperature dependence of the $x(zy)z$ spectrum (E phonons) of $LiTaO_3$ (from Raptis 1988) in the vicinity of the phase transition from ferroelectric to paraelectric; for comparison, the corresponding room-temperature spectrum of ferroelectric $LiTaO_3$ is also given.

polished layer, also shown in figure 6 by data points, agrees quite well with the dependence I_{opt} versus d_p. At the beginning, the intensity decreases slowly. Even after about 0.4 μm of the material is removed, the band intensity is nearly 90% of its original value. Only when the guide becomes too thin to support the fundamental mode, i.e. in the neighbourhood of the mode cut-off, does the intensity of the 69 cm^{-1} band drop abruptly. The experiment shows no evidence of a sublayer in the waveguide surface which could be responsible for the modifications in the Raman spectra.

The main question is what causes the changes in the Raman spectrum of the waveguides. One possible reason might be traced to lattice irregularities introduced in the $LiNbO_3$ crystal by the proton-exchange process. In the present case, the value of x in the chemical formula $Li_{1-x}H_xNbO_3$ is quite high and so is the degree of lattice disorder. In previous studies (Savatinova *et al* 1988, 1990b) a disorder induced background was proposed—a feature representing a measure of the density of vibrational states due to positional, as well as directional, disorder. According to this proposition (Savatinova *et al* 1990b), the Raman spectrum of exchanged crystals contains two components: a background corresponding to a defect-induced partially disordered 'quasi-lattice' (proton-exchange region) and a 'crystalline' component corresponding to the pure (bulk) substrate where the evanescent tail of the optical field penetrates. However, the peak at 69 cm^{-1} is not likely to be caused by defect-induced disorder, as the latter gives a broad continuous rather than a line spectrum and because it has also been weakly observed at room temperature in bulk single crystals in Raman studies of $LiNbO_3$ (Claus *et al* 1972, Penna *et al* 1976b) and $LiTaO_3$ (Raptis 1988).

Other possibilities for the origin of the 69 cm^{-1} line are either (i) that this peak corresponds to a localized vibration caused by traces of heavy impurity atoms introduced in the material during the growth procedure, or (ii) that it represents a one-phonon acoustical mode away from the Brillouin zone centre (most likely at the zone boundary) becoming observable in Raman scattering as a result of the break of symmetry caused by H-doping. In case (i), such impurities produce defects locally which can give a structured (band) first-order Raman spectrum rather than a broad continuum. However, there is no evidence from the literature to substantiate such an argument for the 69 cm^{-1} peak. For either case (i) and (ii), the rate at which the intensity of this peak increases justifies, on the whole, the assumption that it is due to a second-order rather than first-order scattering process.

Because of the weaknesses of the above mentioned interpretations concerning the nature of the 69 cm^{-1} band, we adopt the most likely view that this peak is due to a two-phonon process, and we tentatively suggest the following explanation for the inensity variation of the band in the protonated samples. The idea emerges from the similarity of the Raman spectra of the isomorphous $LiNbO_3$ and $LiTaO_3$ crystals and the recent Raman study of $LiTaO_3$ single crystals over a wide temperature range (Raptis 1988). $LiTaO_3$ becomes paraelectric at 600 °C and the Raman study of its high temperature phase is not difficult. As shown in figure 8, in the high-temperature phase, the number of the observed bands is much smaller than that of the room-temperature phase. The origin of this effect is in the LO–TO splitting which is greatly reduced at high temperature. Because of this, some modes merge with others or decrease in intensity and disappear. The spectral changes occur

in a wide temperature interval below T_c in which the remaining bands broaden and their frequencies become smaller. The picture leads to the conclusion that the phase transition occurs gradually, the process beginning at about 450 °C. In the interval 450–600 °C both phases, ferroelectric and paraelectric, may coexist.

On the basis of the close similarity between the ferroelectric spectra of $LiNbO_3$ and $LiTaO_3$ we can expect similar paraelectric spectra too. In such a case, we can take the risk of considering the spectra of protonated $LiNbO_3$ in figure 4 as a superposition of two parts: a 'quasi-paraelectric' and a 'quasi-ferroelectric' one. It would mean that the process of proton exchange modifies the crystal lattice in the direction of the paraelectric phase. At first sight the idea of a room-temperature paraelectric phase seems rather strange but it is quite possible. Infrared absorption studies of H:$LiNbO_3$ carried out by Savatinova *et al* (1990a), Canali *et al* (1986) and Richter *et al* (1989) have unambiguously demonstrated that the H^-, (OH^-) ions in exchanged layers are situated within the oxide planes, i.e. the protons do not occupy exactly the ferroelectric positions of Li atoms, which are between those planes, but they are shifted towards their paraelectric sites. Thus, the replacement of a lithium ion with a proton results in a displacement of a positive charge along the optical axis. In this situation, one could hardly believe that the protonated lattice would retain the Nb^{5+} and O^{2-} ions in their original positions. It is more likely that these ions would try to restore the equilibrium state of the substance and a common displacement to their non-polar coordinates is one possibility. At high H^- concentrations this could destroy the total ferroelectric balance of the crystal lattice.

The above conception explains in a natural way the absence of electro-optic properties in $LiNbO_3$ protonated layers. After the proton exchange, the electro-optic coefficient r_{33}, which is one of the greatest ones known in the literature, is reduced almost to zero. Special annealing procedures are necessary to restore the coefficient. Parallel to the restoration of r_{33}, the procedure leads to a strong reduction of Δn from 0.12 down to about 0.02. Apparently, the content of hydrogen atoms in the crystal lattice becomes so small that it no longer influences the electro-optic properties of the crystal.

The concept of a 'quasi-paraelectric phase' correlates well with the model proposed by Atuchin (1989) which explains the dependence of the extraordinary refractive index of pure $LiNbO_3$ in terms of the stoichiometry of the crystal. According to this model, the main role in this dependence belongs to the spontaneous polarization of the crystal.

Also our concept does not contradict the x-ray diffraction measurements of powder (Rice 1986) and single-crystal (Ito and Takei 1989) $Li_{1-x}H_xNbO_3$ solid solutions. The analysis reveals a complex structure at high proton concentration consisting of a number of distinct phases along with a variety of phase transitions.

4. Concluding remarks

The Raman spectra of proton exchanged ($H^+ \leftrightarrow Li^+$) $LiNbO_3$ waveguide layers have been measured for various exchange rates corresponding to the guide modes $m = 0$, 1 and 2, and compared with the spectra of the pure (bulk) crystals of $LiNbO_3$ and its isomorphous $LiTaO_3$. The pattern in which the spectra of protonated layers vary with the degree of doping is reminiscent of that of the pure $LiNbO_3$ and $LiTaO_3$ crystals at high temperatures. Irrespective of the origin of the characteristic band at 69 cm^{-1}, which is most likely to be due to second-order Raman scattering and becomes stronger in the direction of increasing doping, it is tentatively suggested that the observed Raman spectra from the protonated layers represent the combined Raman scattering from coexistent ferroelectric and paraelectric $LiNbO_3$ at *room temperature*, with such a phase mixing becoming possible by the proton exchange deformations on the lattice.

Acknowledgments

This work is supported by the Greek General Secretariat for Research and Technology and the Bulgarian Ministry of Research and Technology. We should like to thank Dr Y S Raptis for his participation in part of this work and for useful discussions.

References

Abrahams S C, Levinstein H J and Reddy J M 1966 *J. Phys. Chem. Solids* **27** 1019
Abrahams S C, Buehler E, Hamilton W C and Laplaca S J 1973 *J. Phys. Chem. Solids* **34** 521
Atuchin B b 1989 *Opt. Spektrosk.* **67** 1309
Bergman J C, Ashkin A, Ballman A A, Dziedzic J M, Levinstein H J and Smith R G 1968 *Appl. Phys. Lett.* **12** 92
Canali C, Carnera A, Della Mea G, Mazzoldi P, Al Shukri S M, Nutt A C G and Rue R M 1986 *J. Appl. Phys.* **59** 2643
Chowdhury M R, Peckham G E and Saunderson D H 1978 *J. Phys. C: Solid State Phys.* **11** 1671
Claus R, Borstel G, Wiesendanger E and Steffan L 1972 *Z. Naturf.* **27a** 1187
Gallagher P K and O'Bryan H M Jr 1985 *J. Am. Ceram. Soc.* **68** 147
Ito M and Takei H 1989 *Japan. J. Appl. Phys.* **28** 144
Johnston W D Jr and Kaminow I P 1968 *Phys. Rev.* **168** 1045
Kaminow I P and Johnston W D Jr 1967 *Phys. Rev.* **160** 519
Kolosovskii E A, Petrov D V and Tsaryov A V 1981 *Kvant. Elektron.* **8** 2557
Miller D R, Han O H and Bohn P W 1987 *Appl. Spectrosc.* **41** 249
Noda J, Zembutsu S, Fukunishi S and Uchida N 1978 *Appl. Opt.* **17** 1953
Okamoto Y, Wang Ping-chu and Scott J F 1985 *Phys. Rev.* B **32** 6787
Penna A F, Chaves A and Porto S P S 1976a *Solid State Commun.* **19** 491
Penna A F, Chaves A, Andrade P da R and Porto S P S 1976b *Phys. Rev.* B **13** 4907

Rabolt J F, Santo R and Swalen J D 1980 *Appl. Spectrosc.* **34** 517
Rabolt J F and Swalen J D 1988 *Spectroscopy of Surfaces* ed R J H Clark and R E Hester (New York: Wiley) ch 1
Raptis C 1988 *Phys. Rev.* B **38** 10007
Rice C E 1986 *J. Solid State Chem.* **64** 188
Richter R, Bremer T, Hertel P and Kratzig E 1989 *Phys. Status Solidi* a **114** 765
Savatinova I, Tonchev S, Popov E and Mashev L 1988 *Opt. Commun.* **67** 261
Savatinova I T, Kuneva M, Jordanov B and Kolev D 1990a *J. Mol. Str.* **219** 165
Savatinova I, Kuneva M and Liarokapis E 1990b Electro-Optic and Magneto-Optic Materials II *SPIE Proc.* **1274**
Voronko Yu K, Kudryavtsev A B, Osiko V V, Sobol A A and Sorokin E V 1987 *Sov. Phys.–Solid State* **29** 771
Weis R S and Gaylord T K 1985 *Appl. Phys.* A **37** 191
Wong Ka-Kha 1988 Integrated Optical Circuit Engineering VI *SPIE* **993** 13
Yang X, Lan G, Li B and Wang H 1987 *Phys. Status Solidi* b **142** 287